

# Quantization Under the Real-world Measure: Fast and Accurate Valuation of Long-dated Contracts

Ralph Rudd<sup>1</sup>, Thomas A. McWalter<sup>\*1,2</sup>, Jörg Kienitz<sup>1,3</sup> and Eckhard Platen<sup>1,4</sup>

<sup>1</sup>The African Institute for Financial Markets and Risk Management (AIFMRM),  
University of Cape Town

<sup>2</sup>Department of Finance and Investment Management, University of Johannesburg

<sup>3</sup>Fachbereich Mathematik und Naturwissenschaften, Bergische Universität Wuppertal

<sup>4</sup>Finance Discipline Group and School of Mathematical and Physical Sciences,  
University of Technology Sydney

January 25, 2018

## Abstract

This paper provides a methodology for fast and accurate pricing of the long-dated contracts that arise as the building blocks of insurance and pension fund agreements. It applies the recursive marginal quantization (RMQ) and joint recursive marginal quantization (JRMQ) algorithms outside the framework of traditional risk-neutral methods by pricing options under the real-world probability measure, using the benchmark approach. The benchmark approach is reviewed, and the real-world pricing theorem is presented and applied to various long-dated claims to obtain less expensive prices than suggested by traditional risk-neutral valuation. The growth-optimal portfolio (GOP), the central object of the benchmark approach, is modelled using the time-dependent constant elasticity of variance model (TCEV). Analytic European option prices are derived and the RMQ algorithm is used to efficiently and accurately price Bermudan options on the GOP. The TCEV model is then combined with a 3/2 stochastic short-rate model and RMQ is used to price zero-coupon bonds and zero-coupon bond options, highlighting the departure from risk-neutral pricing.

## 1 Introduction

It has been argued that requiring the existence of a risk-neutral measure is an unrealistic modelling constraint, severe enough to limit the efficacy of long-term pricing and hedging strategies [Hulley and Platen, 2012].

It is, however, possible to derive a unified framework for portfolio optimization, derivative pricing and risk management without the need for an equivalent martingale measure, as described by Platen [2006], the seminal work on the *benchmark approach*. Under this framework, the Law of One Price no longer holds [Platen, 2008], and the Fundamental Theorems of Asset Pricing [Delbaen and Schachermayer, 1994, 1998] do not apply, as the traditional

---

\*Correspondence: tom@analytical.co.za

no-arbitrage concept is relaxed. As a consequence, certain long-dated contracts can be less expensively replicated than suggested by the classical theory.

Central to the benchmark approach is the concept of the growth-optimal portfolio (GOP), first explored by Kelly [1956]. This portfolio strategy is such that, when denoted in units of the GOP, every asset becomes a supermartingale. This allows the derivation of the real-world pricing theorem; yielding the least expensive prices under the real-world probability measure.

The goal of this work is to provide a simple numerical toolbox for the pricing of long-dated contracts under the benchmark approach by using recursive marginal quantization (RMQ). RMQ was introduced by Pagès and Sagna [2015] and is a numerical technique for the optimal approximation of functionals of solutions to stochastic differential equations (SDEs).

The main contribution of this work is two-fold. First, analytic European option prices are derived for the time-dependent constant elasticity of variance (TCEV) model for the GOP. This is an extension of formulae presented by Baldeaux et al. [2014], which generalize the previous option pricing formulae from Miller and Platen [2008, 2010]. Secondly, RMQ is shown to be a highly effective tool for pricing both European options on the GOP, under the assumption of constant interest rates, and zero-coupon bond options, under a stochastic short-rate model, namely the 3/2-model from Ahn and Gao [1999]. This efficient pricing mechanism allows for the wider application of the benchmark approach.

The paper proceeds as follows. In Section 2 the benchmark approach is briefly reviewed in the context of a two-asset scalar diffusion market. The form of the growth-optimal portfolio strategy is specified, and the real-world pricing theorem is derived. The TCEV model is introduced and its probabilistic features are detailed.

In the first part of Section 3, analytic European option pricing formulae are derived for the TCEV model under the assumption of a constant interest rate. The pricing efficiency of these formulae is compared with the approximate prices obtained using RMQ. The latter part of Section 3 deals with stochastic interest rates, specifically the hybrid model introduced by Baldeaux et al. [2015]. Analytic zero-coupon bond prices are presented under the assumption of independence between the stochastic short rate and the GOP. The influence of correlation is briefly explored. Finally, RMQ is used to efficiently price European options on zero-coupon bonds in this framework. Section 4 concludes.

## 2 The Benchmark Approach

This section presents a one-dimensional version of the continuous financial market presented by Platen [2006], similar to the introduction given by Platen and Heath [2006, Chap. 9]. For full mathematical rigor see the original derivation of real-world pricing by Platen [2002], and the extension to the jump-diffusion framework [Platen and Heath, 2006, Chap. 14]. The most general derivation of the “Law of Minimal Price”, of which real-world pricing is a result, is presented by Platen [2008].

Assume the existence of a filtered probability space,  $(\Omega, \mathcal{A}, \underline{\mathcal{A}}, \mathbb{P})$ . The filtration  $\underline{\mathcal{A}} = (\mathcal{A}_t)_{t \in [0, \infty)}$  is assumed to satisfy the usual conditions.

Consider a continuous financial market consisting of two assets: a risk-free savings account,  $S^0 = \{S_t^0, t \in [0, \infty)\}$ , and a risky primary security,  $S^1 = \{S_t^1, t \in [0, \infty)\}$ . They respectively obey the SDEs

$$dS_t^0 = S_t^0 r_t dt \tag{1}$$

and

$$dS_t^1 = S_t^1(a_t dt + b_t dW_t), \quad (2)$$

with  $r = \{r_t, t \in [0, \infty)\}$ , the adapted short rate process. Here  $b = \{b_t, t \in [0, \infty)\}$  is a predictable and strictly positive process known as the diffusion coefficient of  $S^1$  with respect to the standard Brownian motion,  $W$ , and is assumed to satisfy

$$\int_0^T b_s^2 ds < \infty$$

almost surely for  $T \in [0, \infty)$ , a finite time-horizon. It is also assumed that  $a = \{a_t, t \in [0, \infty)\}$ , known as the drift, is a predictable process satisfying

$$\int_0^T |a_s| ds < \infty,$$

almost surely. It is assumed that the SDE (2) has a unique strong solution, see, for example, [Platen and Heath \[2006\]](#).

In the market considered, the number of risky securities is the same as the number of Wiener processes. Refer to [Platen \[2004\]](#) for the case where there are more sources of uncertainty than traded securities.

Defining the market price of risk (MPOR) process as

$$\theta_t := b_t^{-1}(a_t - r_t),$$

allows the SDE (2) to be re-written as

$$dS_t^1 = S_t^1((r_t + b_t \theta_t) dt + b_t dW_t). \quad (3)$$

It is assumed that the absolute value of the MPOR process is always finite.

## 2.1 The Growth Optimal Portfolio

The GOP has often been attributed to [Kelly \[1956\]](#). [Hakansson and Ziemba \[1995\]](#) state in their review of the growth optimal investment strategy that the GOP was already implied by Bernoulli's solution to the St. Petersburg Paradox as early as 1738 (see [Samuelson \[1977\]](#) for this interesting digression). An important application of the GOP to claim valuation and long-run portfolio growth is [Long \[1990\]](#), where it is shown that, under certain constraints, risk-neutral pricing is equivalent to pricing under the real-world probability measure using the GOP as the numeraire.

The GOP is the central object of the benchmark approach and hence real-world pricing. In a general semimartingale framework, [Karatzas and Kardaras \[2007\]](#) show that the “no unbounded profit with bounded risk” no-arbitrage condition is necessary and sufficient for the existence of the GOP. This condition is placed into its proper context alongside the range of applicable arbitrage statements by [Fontana \[2015\]](#).

In the market defined above, a predictable stochastic vector process  $\delta = \{\delta_t = (\delta_t^0, \delta_t^1), t \in [0, T]\}$  is called a *strategy* if, for all  $t \in [0, T]$ , the stochastic Itô integrals

$$\int_0^t \delta_s^0 dS_s^0 \quad \text{and} \quad \int_0^t \delta_s^1 dS_s^1$$

exist. Denote by  $S^\delta = \{S_t^\delta, t \in [0, T]\}$  the time- $t$  value of the portfolio process associated with the strategy  $\delta$ , defined as

$$S_t^\delta = \delta_t^0 S_t^0 + \delta_t^1 S_t^1.$$

A strategy and its corresponding portfolio process are said to be self-financing if

$$dS_t^\delta = \delta_t^0 dS_t^0 + \delta_t^1 dS_t^1,$$

for all  $t \in [0, T]$ . The self-financing condition ensures that instantaneous changes in the value of the portfolio are due to changes in the prices of the constituent securities and not to external deposits or withdrawals. Only self-financing portfolios are considered in the following.

At this point it is necessary to introduce the concept of *admissible* portfolios, to avoid the arbitrage opportunities generated by traditional doubling strategies. Admissible strategies are usually either constrained via an absolute lower bound or an integrability condition (see [Hunt and Kennedy \[2004, Chap. 7\]](#) for a discussion). Only the set,  $\mathcal{V}^+$ , of strictly positive portfolios will be considered, thus providing an absolute lower bound at zero. For  $S^\delta \in \mathcal{V}^+$ , define the portfolio fraction

$$\pi_{\delta,t}^j = \frac{\delta_t^j S_t^j}{S_t^\delta},$$

as the fraction of the total portfolio value invested in each asset,  $S_t^j$ , for  $j \in \{0, 1\}$ . Portfolio fractions can be negative but must always sum to one. Using (3), the SDE for a self-financing portfolio in  $\mathcal{V}^+$  can now be written as

$$dS_t^\delta = S_t^\delta \left( (r_t + \pi_{\delta,t}^1 b_t \theta_t) dt + \pi_{\delta,t}^1 b_t dW_t \right).$$

A simple application of Itô's formula provides the SDE for the logarithm of the portfolio

$$d \log S_t^\delta = g_{\delta,t} dt + \pi_{\delta,t}^1 b_t dW_t,$$

with portfolio growth rate

$$g_{\delta,t} = r_t + \pi_{\delta,t}^1 b_t \theta_t - \frac{1}{2} (\pi_{\delta,t}^1 b_t)^2. \quad (4)$$

The GOP is the portfolio that maximises this growth rate, that is, the drift of the log-portfolio. Mathematically, a strictly positive portfolio value process,  $S^{\delta^*} = \{S_t^{\delta^*}, t \in [0, T]\}$ , is a growth optimal portfolio if, for all  $t \in [0, T]$  and all  $S^\delta \in \mathcal{V}^+$ , the inequality

$$g_{\delta^*,t} \geq g_{\delta,t}$$

holds almost surely. From the first-order condition for the maximum of the growth rate (4), the optimal fraction to be invested in  $S^1$  can be found as

$$\pi_{\delta^*,t}^1 = b_t^{-1} \theta_t.$$

Consequently the SDE for the GOP is given by

$$dS_t^{\delta^*} = S_t^{\delta^*} \left( (r_t + \theta_t^2) dt + \theta_t dW_t \right), \quad (5)$$

with  $t \in [0, T]$  and  $S_0^{\delta^*} > 0$ . Contingent claims can now be priced under the real-world probability measure using the GOP as the numeraire or *benchmark*, as will be detailed below.

## 2.2 Real-world Pricing

Using the GOP as benchmark and numeraire, consider the evolution of a benchmarked portfolio given by the ratio

$$\hat{S}_t^\delta = \frac{S_t^\delta}{S_t^{\delta*}}.$$

Itô's formula provides the SDE

$$d\hat{S}_t^\delta = (\delta_t^1 \hat{S}_t^1 b_t - \hat{S}_t^\delta \theta_t) dW_t, \quad (6)$$

in terms of  $\hat{S}_t^1 = \frac{S_t^1}{S_t^{\delta*}}$ , the benchmarked security price process.

Because no drift is present in (6), it is clear that benchmarked portfolios form  $(\mathcal{A}, \mathbb{P})$ -local martingales. Thus, by Fatou's lemma, all non-negative portfolios, when benchmarked, are  $(\mathcal{A}, \mathbb{P})$ -supermartingales<sup>1</sup>.

Define a non-negative contingent claim,  $V_\tau$ , that matures at a stopping time  $\tau \in [0, T]$ , as an  $\mathcal{A}_\tau$ -measurable payoff that possesses a finite expectation when benchmarked. Note that  $V_\tau$  need not be square-integrable. Let  $S_t^V$  denote a non-negative self-financing portfolio that replicates the claim, i.e.,  $S_\tau^V = V_\tau$ . Then

$$\frac{S_t^V}{S_t^{\delta*}} \geq \mathbb{E} \left[ \frac{V_T}{S_T^{\delta*}} \middle| \mathcal{A}_t \right]$$

holds by the supermartingale property of benchmarked non-negative self-financing portfolios.

A security price process, equivalent to a self-financing, replicating portfolio, is called *fair* if its benchmarked value forms an  $(\mathcal{A}, \mathbb{P})$ -martingale (in the classical risk-neutral setting, this notion of a fair process is equivalent to that proposed by Geman et al. [1995]). Under the benchmark approach this leads to the minimal possible price, the desired result for this section.

**Theorem 2.1** (Real-world Pricing). *For any fair security price process,  $V = \{V_t, t \in [0, T]\}$ ,  $T \in (t, \infty)$ , one has the real-world pricing formula*

$$V_t = S_t^{\delta*} \mathbb{E} \left[ \frac{V_T}{S_T^{\delta*}} \middle| \mathcal{A}_t \right]. \quad (7)$$

The expectation in Theorem 2.1 is taken under the real-world probability measure,  $\mathbb{P}$ . Under the assumption that one can perform an equivalent probability measure change, following Geman et al. [1995], the candidate Radon-Nikodym derivative process to move from the current real-world numeraire-measure pair,  $(S^{\delta*}, \mathbb{P})$ , to the risk-neutral numeraire-measure pair,  $(S^0, \mathbb{P}_\theta)$ , is

$$\lambda_\theta(t) = \frac{d\mathbb{P}_\theta}{d\mathbb{P}} \bigg|_{\mathcal{A}_t} = \frac{S_t^0 S_0^{\delta*}}{S_0^0 S_t^{\delta*}} = \frac{\hat{S}_t^0}{\hat{S}_0^0}. \quad (8)$$

If  $\lambda_\theta(t)$  is a strictly positive  $(\mathcal{A}, \mathbb{P})$ -martingale (and not a strict local-martingale), then the probability measure change can indeed be performed, yielding

$$V_t = S_t^{\delta*} \mathbb{E} \left[ \frac{V_T}{S_T^{\delta*}} \middle| \mathcal{A}_t \right] = \mathbb{E} \left[ \frac{\lambda_\theta(T) S_t^0}{\lambda_\theta(t) S_T^0} V_T \middle| \mathcal{A}_t \right] = \mathbb{E}_\theta \left[ \frac{S_t^0}{S_T^0} V_T \middle| \mathcal{A}_t \right],$$

<sup>1</sup>For a simple proof of this classic result, see Platen and Heath [2006, Lemma 5.2.3].

by Bayes' theorem, where the last expression is the classical risk-neutral pricing formula.

In this way, risk-neutral pricing is a special case of real-world pricing, applicable only when  $\lambda_\theta(t)$  describes a strictly positive  $(\mathcal{A}, \mathbb{P})$ -martingale. This translates into a constraint on the market price of risk  $\theta_t$ , the volatility of the GOP. This volatility must be specified so that  $\lambda_\theta(t)$  is a martingale, which is, for instance, the case if  $\theta_t$  satisfies Novikov's condition or, more generally, Kazamaki's condition [Revuz and Yor, 1999]. To compute the expectation in Theorem 2.1, the GOP must be modelled explicitly. A realistic model for the GOP, which excludes risk-neutral pricing, is presented in the next section.

### 2.3 Modelling the GOP

Consider a simple two-asset market consisting only of the risk-free bank account and the growth-optimal portfolio, obeying (1) and (5), respectively. The *discounted* GOP is then described by

$$\bar{S}_t^* = \frac{S_t^*}{S_t^0},$$

which means that

$$d\bar{S}_t^* = \bar{S}_t^* (\theta_t^2 dt + \theta_t dW_t).$$

The  $\delta_*$ -superscript has been dropped from the GOP notation for simplicity. To compute the expectation in (7), the MPOR process,  $\theta_t$ , must be modelled explicitly.

Baldeaux et al. [2014] propose the TCEV model for the GOP. It is parsimonious, tractable, reliably estimated and can provide explicit formulae for various derivatives and their hedge ratios. The TCEV model is specified by

$$\theta_t := c \left( \frac{\bar{S}_t^*}{\alpha_t} \right)^{a-1} \quad \text{and} \quad \alpha_t := \alpha_0 e^{\eta t}.$$

Here the parameter restrictions are  $c > 0$ ,  $a \in (-\infty, 1)$ ,  $\alpha_0 > 0$  and  $\eta > 0$ . Note that the TCEV model generalizes both the minimal market model (MMM), first introduced by Platen [2001] and analyzed in detail by Miller and Platen [2008], and the modified constant elasticity of variance model (MCEV) from Heath and Platen [2002].

By direct substitution, the SDE for the discounted GOP under the TCEV model is

$$d\bar{S}_t^* = c^2 \alpha_t^{2(1-a)} (\bar{S}_t^*)^{2a-1} dt + c \alpha_t^{1-a} (\bar{S}_t^*)^a dW_t. \quad (9)$$

The behaviour of this process is described by Proposition 2.2 below, which appears in a slightly modified form in Baldeaux et al. [2014].

**Proposition 2.2.** *The process  $\bar{S}^* = \{\bar{S}_t^*, t \geq 0\}$  satisfies the following equality in distribution*

$$\bar{S}_t^* \stackrel{(d)}{=} X_{\varphi(t)}^{\frac{1}{2(1-a)}} = X_{\varphi(t)}^{\left(\frac{\delta}{2}-1\right)},$$

where  $X = \{X_\varphi, \varphi \geq 0\}$  is a squared Bessel process of dimension  $\delta = \frac{3-2a}{1-a}$  in  $\varphi$ -time and the time-transformation is given by

$$\varphi(t) = \frac{(1-a)\alpha_0^{2(1-a)}c^2}{2\eta} \left( e^{2(1-a)\eta t} - 1 \right).$$

*Proof.* Define  $Y_t = \left(\frac{\alpha_0}{\alpha_t} \bar{S}_t^*\right)^{2(1-a)}$  such that

$$dY_t = \left(\alpha_0^{2(1-a)} c^2 (1-a)(3-2a) - 2(1-a)\eta Y_t\right) dt + 2(1-a)\alpha_0^{1-a} c \sqrt{Y_t} dW_t.$$

This is a CIR-process and thus by Proposition A.1, in Appendix A,

$$Y_t = e^{-2(1-a)\eta t} X_{\varphi(t)}.$$

Since  $\bar{S}_t^* = e^{\eta t} Y_t^{\frac{1}{2(1-a)}}$ , this completes the proof.  $\square$

An immediate consequence of the relationship between the discounted GOP and a squared Bessel process (BESQ) of dimension  $\delta = \frac{3-2a}{1-a} > 2$ , is that the discounted GOP never attains zero (see Appendix A.1). A more subtle consequence is that modelling the GOP portfolio in this way precludes the existence of an equivalent risk-neutral probability measure.

As in Section 2.2, the candidate Radon-Nikodym derivative process to move to the risk-neutral measure is given by (8). However, now

$$\hat{S}_t^0 = \frac{1}{\bar{S}_t^*} = X_{\varphi(t)}^{1-\frac{\delta}{2}},$$

and from the symmetry relationship derived for BESQ processes in Appendix A.1, the process on the right-hand side of the above expression is a *strict* local martingale. Thus, the ‘risk-neutral measure’ induced by this Radon-Nikodym derivative process will not be a probability measure.

Alternatively, consider the existence of a measure,  $\mathbb{P}_\theta$ , such that the discounted GOP is potentially a martingale under this measure,

$$d\bar{S}_t^* = c\alpha_t^{1-a} (\bar{S}_t^*)^a dW_t^\theta. \quad (10)$$

Using the same transformation as in the proof of Proposition 2.2,  $Y_t = \left(\frac{\alpha_0}{\alpha_t} \bar{S}_t^*\right)^{2(1-a)}$ , it is straightforward to show that under this hypothetical measure the discounted GOP is the power of a BESQ process of dimension  $\delta_\theta = \frac{1-2a}{1-a} < 2$ . As this process has a non-zero probability of attaining zero in finite time, the measure  $\mathbb{P}_\theta$  cannot be equivalent to  $\mathbb{P}$ , the original real-world probability measure under which  $X$  has dimension  $\delta = \frac{3-2a}{1-a} > 2$  and never hits zero.

### 3 Option Pricing

In this section, recursive marginal quantization is used to provide fast and accurate pricing for the benchmark approach. RMQ was introduced by Pagès and Sagna [2015], and extended to higher-order schemes by McWalter et al. [2018].

Initially, analytic European option prices are derived under the assumption of constant interest rates. These formulae generalize those found in Miller and Platen [2008, 2010] for the minimal market and modified constant elasticity of variance models, respectively. Although these formulae are analytic, they can be numerically expensive to compute and are contrasted to the fast, but approximate, prices obtained via RMQ. Furthermore, Bermudan options on

the GOP are priced using traditional Monte Carlo methods, with their accuracy, speed and efficiency compared with that of recursive marginal quantization.

The second subsection deals with the hybrid model introduced by [Baldeaux et al. \[2015\]](#). The hybrid model combines the TCEV model for the GOP with a 3/2 stochastic short-rate model. [Baldeaux et al. \[2015\]](#) derive analytic zero-coupon bond prices under the assumption that the GOP is independent of the short rate. In this section, numerical experiments show that these prices are well approximated with RMQ. The effect of the independence assumption on the zero-coupon bond prices is also investigated. Lastly, European options on zero-coupon bonds are priced using both traditional Monte Carlo methods as well as RMQ.

All simulations were performed using MATLAB 2016b on a computer with a 2.00 GHz Intel i-3 processor and 4 GB of RAM.

### 3.1 Constant Short Rates

Expressions similar to those derived in Propositions 3.1 and 3.2 below appear in [Baldeaux et al. \[2014\]](#), where the strike was selected to be a constant multiple of the savings account. In this way, [Baldeaux et al. \[2014\]](#) were able to avoid specifying a model for the short rate by restricting the class of strikes they considered.

**Proposition 3.1.** *Assuming a constant interest rate  $r$ , the real-world price,  $p_{T,K}(t, S_t^*)$ , of a European put option on the GOP at time  $t$  with expiry  $T$  and strike  $K$  is given by*

$$p_{T,K}(t, S_t^*) = -\bar{S}_t^* \beta(t) \chi'^2 \left( \frac{\tilde{K}}{\Delta\varphi}; \delta, \frac{(\bar{S}_t^*)^{2(1-a)}}{\Delta\varphi} \right) + K \frac{\beta(t)}{\beta(T)} \left[ \chi'^2 \left( \frac{(\bar{S}_t^*)^{2(1-a)}}{\Delta\varphi}; \delta - 2, 0 \right) - \chi'^2 \left( \frac{(\bar{S}_t^*)^{2(1-a)}}{\Delta\varphi}; \delta - 2, \frac{\tilde{K}}{\Delta\varphi} \right) \right],$$

where

$$\begin{aligned} \tilde{K} &= \left( \frac{K}{\beta(T)} \right)^{2(1-a)}, & \beta(t) &= \exp(rt), \\ \delta &= \frac{3-2a}{1-a}, & \Delta\varphi &= \varphi(T) - \varphi(t), \end{aligned}$$

with  $\chi'^2(x; \delta, \lambda)$  representing the noncentral chi-squared distribution, evaluated at  $x$  with degrees of freedom  $\delta$  and non-centrality parameter  $\lambda$ , and  $\varphi(t)$  is defined in Proposition 2.2.

*Proof.* When the short rate is constant, the savings account is deterministic, with

$$S_t^0 = \exp(rt) =: \beta(t).$$

As is standard, the expectation of the numeraire denominated payoff can be expressed as the difference of two expectations,

$$\begin{aligned} p_{T,K}(t, S_t^*) &= \mathbb{E} \left[ \frac{S_t^*}{S_T^*} (K - S_T^*)^+ \middle| \mathcal{A}_t \right] \\ &= \mathbb{E} \left[ \frac{\bar{S}_t^*}{\bar{S}_T^*} \beta(t) \left( \frac{K}{\beta(T)} - \bar{S}_T^* \right)^+ \middle| \mathcal{A}_t \right] \\ &= \bar{S}_t^* \frac{\beta(t)}{\beta(T)} K \mathbb{E} \left[ \frac{1}{\bar{S}_T^*} \mathbb{I}_{\left\{ \frac{K}{\beta(T)} > \bar{S}_T^* \right\}} \middle| \mathcal{A}_t \right] - \bar{S}_t^* \beta(t) \mathbb{E} \left[ \mathbb{I}_{\left\{ \frac{K}{\beta(T)} > \bar{S}_T^* \right\}} \middle| \mathcal{A}_t \right]. \end{aligned}$$



Using Proposition 2.2, the first expectation can be rewritten in terms of the power of a squared Bessel process of dimension  $\delta = \frac{3-2a}{1-a} > 2$ ,

$$\begin{aligned}\mathbb{E}\left[\frac{1}{\bar{S}_t^*} \mathbb{I}_{\left\{\frac{K}{\beta(T)} > \bar{S}_T^*\right\}} \middle| \mathcal{A}_t\right] &= \mathbb{E}\left[X_{\varphi(T)}^{-\left(\frac{\delta}{2}-1\right)} \mathbb{I}_{\{\tilde{K} > X_{\varphi(T)}\}} \middle| \mathcal{A}_t\right] \\ &= \int_0^{\tilde{K}} X^{-\left(\frac{\delta}{2}-1\right)} p_{\delta>2}(X, \varphi(T); X_{\varphi(t)}) dX,\end{aligned}$$

with the transition density,  $p_{\delta>2}$ , given by (23) in Appendix A. Now, the symmetry relationship, (26) in Appendix A, can be applied to yield

$$\int_0^{\tilde{K}} X^{-\left(\frac{\delta}{2}-1\right)} p_{\delta>2}(X, \varphi(T); X_{\varphi(t)}) dX = X_{\varphi(t)}^{-\left(\frac{\delta}{2}-1\right)} \int_0^{\tilde{K}} p_{4-\delta}(X, \varphi(T); X_{\varphi(t)}) dX,$$

where the final density to be integrated is the norm-decreasing density given by (17). The bounds can be rewritten as

$$\begin{aligned}X_{\varphi(t)}^{-\left(\frac{\delta}{2}-1\right)} \int_0^{\tilde{K}} p_{4-\delta}(X, \varphi(T); X_{\varphi(t)}) dX &= \\ \frac{1}{\bar{S}_t^*} \left[ \int_0^\infty p_{4-\delta}(X, \varphi(T); X_{\varphi(t)}) dX - \int_{\tilde{K}}^\infty p_{4-\delta}(X, \varphi(T); X_{\varphi(t)}) dX \right],\end{aligned}$$

and using (19) and (20) from the Appendix gives

$$\mathbb{E}\left[\frac{1}{\bar{S}_t^*} \mathbb{I}_{\left\{\frac{K}{\beta(T)} > \bar{S}_T^*\right\}} \middle| \mathcal{A}_t\right] = \frac{1}{\bar{S}_t^*} \left[ \chi'^2 \left( \frac{(\bar{S}_t^*)^{2(1-a)}}{\Delta\varphi}; \delta - 2, 0 \right) - \chi'^2 \left( \frac{(\bar{S}_t^*)^{2(1-a)}}{\Delta\varphi}; \delta - 2, \frac{\tilde{K}}{\Delta\varphi} \right) \right].$$

Similarly, the second expectation can be computed directly from the transition density (23),

$$\begin{aligned}\mathbb{E}\left[\mathbb{I}_{\left\{\frac{K}{\beta(T)} > \bar{S}_T^*\right\}} \middle| \mathcal{A}_t\right] &= \int_0^{\tilde{K}} p_{\delta>2}(X, \varphi(T); X_{\varphi(t)}) dX \\ &= \chi'^2 \left( \frac{\tilde{K}}{\Delta\varphi}; \delta, \frac{(\bar{S}_t^*)^{2(1-a)}}{\Delta\varphi} \right).\end{aligned}$$

□

The analytic expression for the European call option can be derived in the same way, but the derivation avoids the norm-decreasing density required above.

**Proposition 3.2.** *Assuming a constant interest rate  $r$ , the real-world price,  $c_{T,K}(t, S_t^*)$ , of a European call option on the GOP at time  $t$  with expiry  $T$  and strike  $K$  is given by*

$$c_{T,K}(t, S_t^*) = \bar{S}_t^* \beta(t) \left[ 1 - \chi'^2 \left( \frac{\tilde{K}}{\Delta\varphi}; \delta, \frac{(\bar{S}_t^*)^{2(1-a)}}{\Delta\varphi} \right) \right] - K \frac{\beta(t)}{\beta(T)} \chi'^2 \left( \frac{(\bar{S}_t^*)^{2(1-a)}}{\Delta\varphi}; \delta - 2, \frac{\tilde{K}}{\Delta\varphi} \right),$$

with all definitions as in Proposition 3.1.

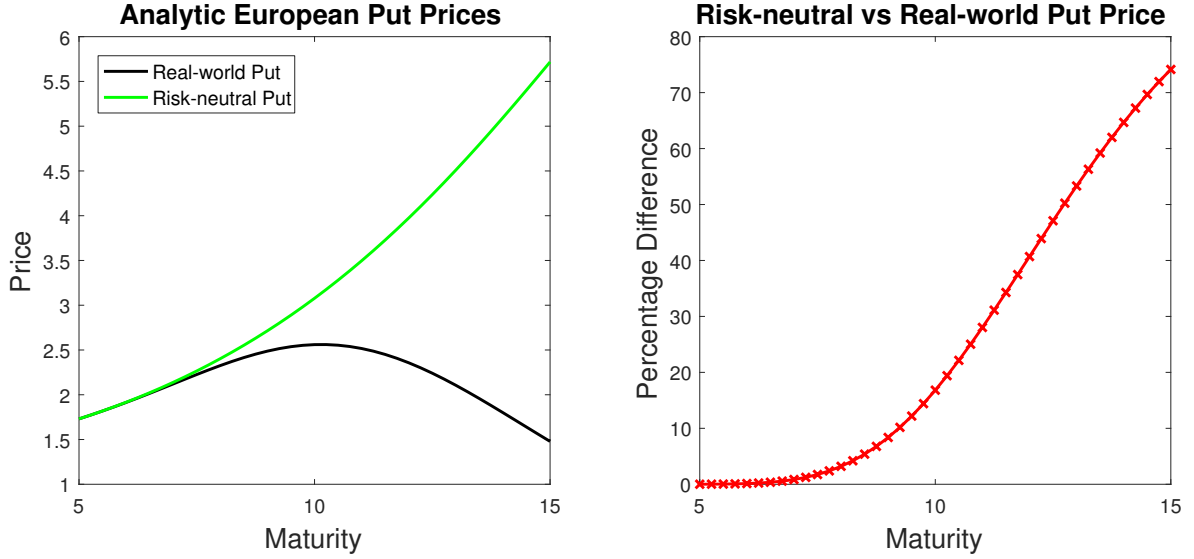


Figure 1: Comparison of risk-neutral and real-world prices obtained for at-the-money European put options with maturities out to 15 years.

For comparison, assume a hypothetical risk-neutral measure,  $\mathbb{P}_\theta$ , with the discounted GOP dynamics under this measure given by (10). Although this measure is not equivalent to  $\mathbb{P}$ , when the strike  $K > 0$ , the risk-neutral call price, denoted  $c_{T,K}^{\text{RN}}$ , corresponds to the real-world call price given above for  $\delta_\theta = \frac{1-2a}{1-a}$ . This occurs because the measures differ only for values of  $S^*$  around 0, which the integral in the call pricing problem avoids for positive strikes. However, the risk-neutral put option, denoted  $p_{T,K}^{\text{RN}}$ , is significantly more expensive than the real-world put option for long time horizons.

To see this, consider the mathematical basis for put-call parity,

$$(K - S_T^+)^+ = (S_T^* - K)^+ - S_T^* + K. \quad (11)$$

Taking the expectation under the real-world measure, with the GOP as the numeraire, provides the *fair* put-call parity relationship,

$$p_{T,K}(t, S_t^*) = c_{T,K}(t, S_t^*) - S_t^* + K P_T(t, S_t^*),$$

where the fair or real-world zero coupon bond price is given by

$$P_T(t, S_t^*) = \mathbb{E} \left[ \frac{S_T^*}{S_t^*} \middle| \mathcal{A}_t \right] = \frac{\beta(t)}{\beta(T)} \mathbb{E} \left[ \frac{\bar{S}_T^*}{\bar{S}_t^*} \middle| \mathcal{A}_t \right] = \frac{\beta(t)}{\beta(T)} \chi'^2 \left( \frac{(\bar{S}_t^*)^{2(1-a)}}{\Delta\varphi}; \delta - 2, 0 \right).$$

Of course, taking the discounted risk-neutral expectation of (11) provides the classical put-call parity relationship,

$$p_{T,K}^{\text{RN}}(t, S_t^*) = c_{T,K}^{\text{RN}}(t, S_t^*) - S_t^* + K \frac{\beta(t)}{\beta(T)}.$$

Since the hypothetical risk-neutral call prices and real-world call prices coincide, and

$$P_T(t, S_t^*) \leq \frac{\beta(t)}{\beta(T)},$$

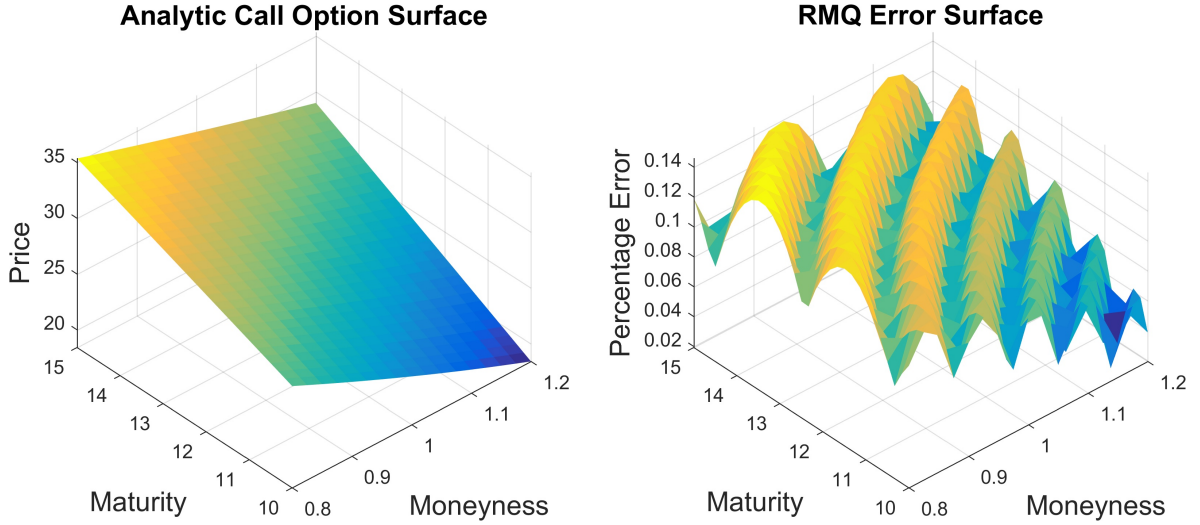


Figure 2: European call option price surface with RMQ pricing error.

the real-world put option prices must be less than or equal to the risk-neutral put option prices.

Figure 1 illustrates the difference between long-dated at-the-money put options priced using the classical risk-neutral pricing theory and the prices provided by Proposition 3.1, obtained using real-world pricing. The parameters used are taken from Baldeaux et al. [2015], where they were estimated from empirical data, with  $\alpha_0 = 51.34$ ,  $\eta = 0.1239$ ,  $c = 0.1010$  and  $a = 0.2868$ . The initial discounted GOP was set at 50 and the constant short rate at 5%. Maturities are set at bi-monthly intervals from 5 out to 15 years.

The left panel of Figure 1 shows how the prices correspond for short maturities, with the risk-neutral put becoming more and more expensive as the maturities lengthen. The right panel of Figure 1 shows the difference between the risk-neutral put and the real-world put as a percentage of the classical risk-neutral option price. At a maturity of 15 years, the real-world put option is 70% less expensive to purchase.

As a first example of RMQ, Figure 2 shows an analytic European call option pricing surface along with the RMQ pricing error. Moneyness is varied by changing the strike over the initial GOP value, and maturities are set at monthly intervals from 10 to 15 years.

The weak order 2.0 RMQ scheme was used [McWalter et al., 2018] with 12 time-steps per year and 50 codewords held constant across time. The final error is under 0.15% irrespective of maturity and moneyness. The error oscillates across moneyness, as is expected for a tree-type method. Computing the RMQ grid out to 15 years takes less than 1 second.

In Figure 3, Bermudan put options on the GOP with a maturity of 5 years and monthly exercise opportunities are priced using both a least-squares Monte Carlo simulation and RMQ. The Monte Carlo simulation is a 500 000 path long-step simulation, using the exact transition density of the discounted GOP. The RMQ algorithm is again the weak order 2.0 scheme with 12 time-steps and 100 codewords. The Monte Carlo algorithm takes approximately 14.9 seconds per strike, whereas the RMQ algorithm takes only 0.5 seconds to price all strikes. The maximum difference between the two methods is 1.4% of the price in the worst case. Thus, the methods agree very well across strikes with the RMQ algorithm being significantly faster

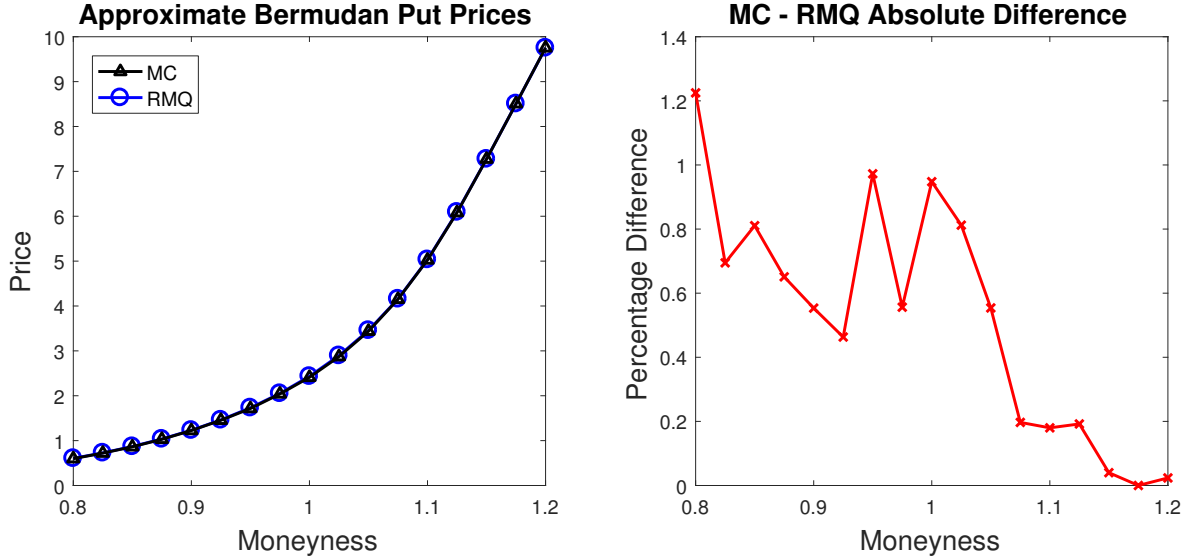


Figure 3: Bermudan put options priced using least-squares Monte Carlo and RMQ.

to compute. Note that the RMQ results may well be more accurate than the least-squares Monte Carlo results for low moneyness, as the Monte Carlo simulation may be unreliable for deep out-the-money options.

### 3.2 Stochastic Short Rates

In this subsection, the hybrid model, investigated by [Baldeaux et al. \[2015\]](#), is extended by relaxing the assumption of independence between the short rate and the discounted GOP. It is shown how the real-world zero-coupon bond prices become significantly less than risk-neutral prices as maturities increase. Fast and accurate numerical pricing for European put options on zero-coupon bonds is also provided.

[Baldeaux et al. \[2015\]](#) undertake an empirical investigation to determine which short-rate model, combined with the TCEV model for the discounted GOP, performs best when pricing and hedging long-dated zero-coupon bonds. Their investigation concluded that the 3/2 short-rate model of [Ahn and Gao \[1999\]](#) outperforms the competing models in terms of capturing the dynamics of the real-world short-term interest rate, as well as delivering the smallest prices for zero-coupon bonds.

Under the real-world measure, the 3/2 short-rate model is described by

$$dr_t = \kappa(\theta r_t - r_t^2) dt + \sigma r_t^{3/2} dW_t^r, \quad (12)$$

with  $r_0 > 0$ . Proposition 3.3 below is reproduced from [Baldeaux et al. \[2015\]](#).

**Proposition 3.3.** *If the Brownian motion,  $W^r$ , driving the short rate is independent of the Brownian motion,  $W$ , driving the GOP then the time- $t$  price of a fair zero-coupon bond maturing at  $T$  is given by*

$$P_T(t, r_t, \bar{S}_t^*) = \mathbb{E} \left[ \frac{S_t^*}{S_T^*} \middle| \mathcal{A}_t \right] = \mathbb{E} \left[ \frac{\bar{S}_t^* S_t^0}{\bar{S}_T^* S_T^0} \middle| \mathcal{A}_t \right] = M(\bar{S}_t^*, t, T) G(r_t, t, T), \quad (13)$$

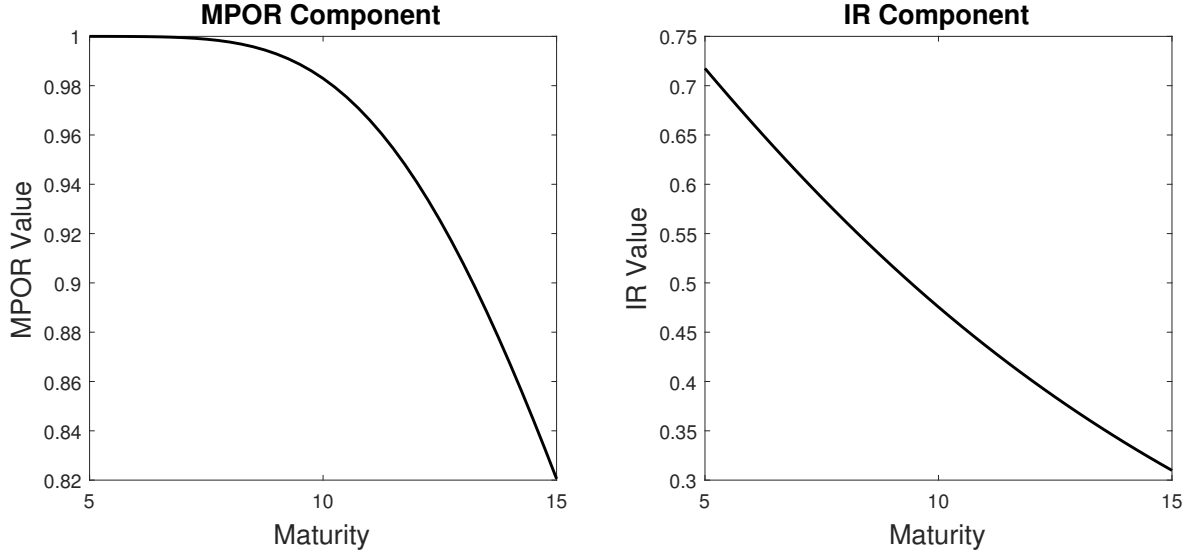


Figure 4: The analytic MPOR and IR components of the fair zero-coupon bond price under the hybrid model.

with

$$M(\bar{S}_t^*, t, T) = \mathbb{E} \left[ \frac{\bar{S}_t^*}{\bar{S}_T^*} \middle| \mathcal{A}_t \right] = \chi'^2 \left( \frac{(\bar{S}_t^*)^{2(1-a)}}{\Delta\varphi}; \delta - 2, 0 \right) \quad (14)$$

denoting the market price of risk component and

$$G(r_t, t, T) = \mathbb{E} \left[ \frac{S_t^0}{S_T^0} \middle| \mathcal{A}_t \right] = \mathbb{E} \left[ \exp \left( \int_t^T r_s ds \right) \middle| \mathcal{A}_t \right] \quad (15)$$

denoting the interest-rate (IR) component.

*Proof.* The independence of the GOP from the short rate, and thus the savings account, allows the expectation in (13) to be separated into the product of (14) and (15). The right-hand side of (14) follows directly from the known transition density of the discounted GOP, provided by Proposition 2.2, and the right-hand side of (15) follows from the definition of the savings account, (1).  $\square$

As a result of the above proposition, if the expectation in (15) was taken under the risk-neutral measure, the fair zero-coupon bond price could be interpreted as the product of the traditional risk-neutral bond price,  $G(r_t, t, T)$ , and the market price of risk component,  $M(\bar{S}_t^*, t, T)$ . Note that the MPOR component is given explicitly as the probability that all paths of the inverse discounted GOP process have not attained zero by time  $T$ . This probability goes to 0 as  $T$  goes to infinity; eventually the growth-optimal portfolio dominates any other traded asset, ensuring that the expected value of the asset, expressed in terms of the GOP, goes to zero.

This behaviour can be seen in the left panel of Figure 4, where the MPOR component is plotted out to 15 years using the model parameters in the previous section. Note that the

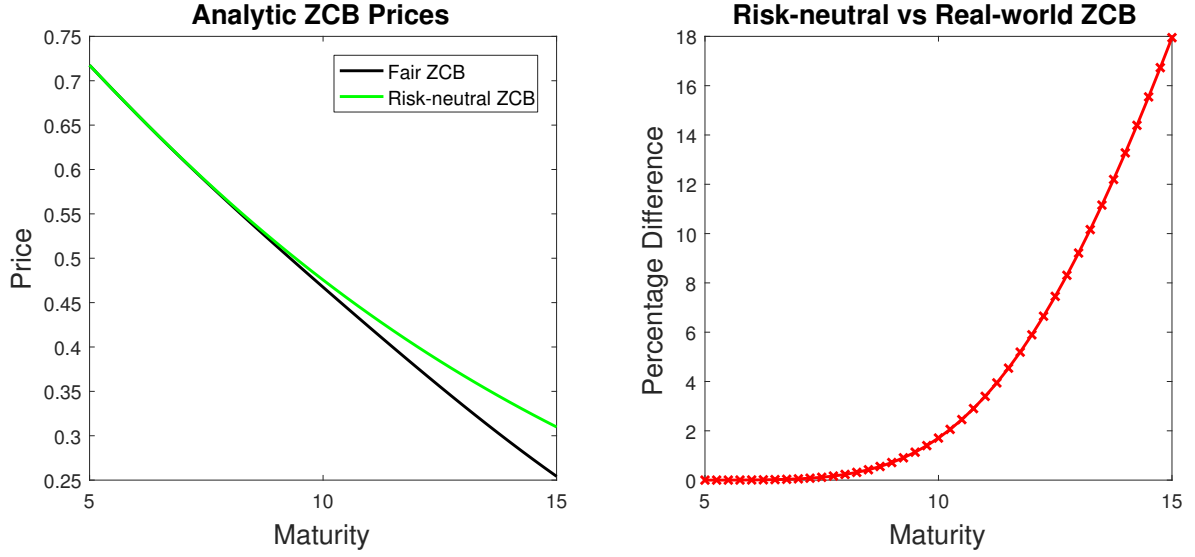


Figure 5: The analytic fair zero-coupon bond price in the hybrid model compared to the hypothetical risk-neutral bond price for maturities ranging from 5 to 15 years.

MPOR component only becomes significantly less than one well after the 5-year mark. This indicates that theoretical real-world bond prices and those obtained using classical risk-neutral pricing would coincide for maturities out to roughly 8 years for these parameters.

**Proposition 3.4.** *Under the 3/2 short-rate model,*

$$G(r_t, t, T) = \frac{\Gamma(\alpha - \gamma)x(r_t, t, T)^\gamma}{\Gamma(\alpha)} {}_1F_1(\gamma, \alpha, -x(r_t, t, T))$$

with

$$\begin{aligned} \alpha &= \frac{2}{\sigma^2} (\kappa + (1 + \gamma)\sigma^2), & \gamma &= \frac{1}{\sigma^2} (\sqrt{\phi^2 + 2\sigma^2} - \phi) \\ x(r, t, T) &= \frac{2\kappa\theta}{\sigma^2 (e^{\kappa\theta(T-t)} - 1)r}, & \phi &= \kappa + \frac{1}{2}\sigma^2, \end{aligned}$$

and where  ${}_1F_1$  is the confluent hypergeometric function of the first kind, or Kummer's function.

*Proof.* See [Ahn and Gao \[1999, Sec. 3\]](#). □

The IR component is illustrated in the right panel of Figure 4, using the 3/2 model parameters estimated from the market by [Baldeaux et al. \[2015\]](#), with  $\kappa = 3.5726$ ,  $\theta = 0.096$ ,  $\sigma = 0.7960$  and the initial short rate selected as  $r_0 = 0.05$ .

Finally, the analytic fair zero-coupon bond price is displayed in Figure 5 for maturities out to 15 years and contrasted with the risk-neutral bond price. The right panel of Figure 5 shows the difference between the hypothetical risk-neutral bond and the real-world bond as a percentage of the classical risk-neutral bond price. At a maturity of 15 years, the fair bond is 18% less expensive to purchase. It is clear that the fair bond will continue to become less

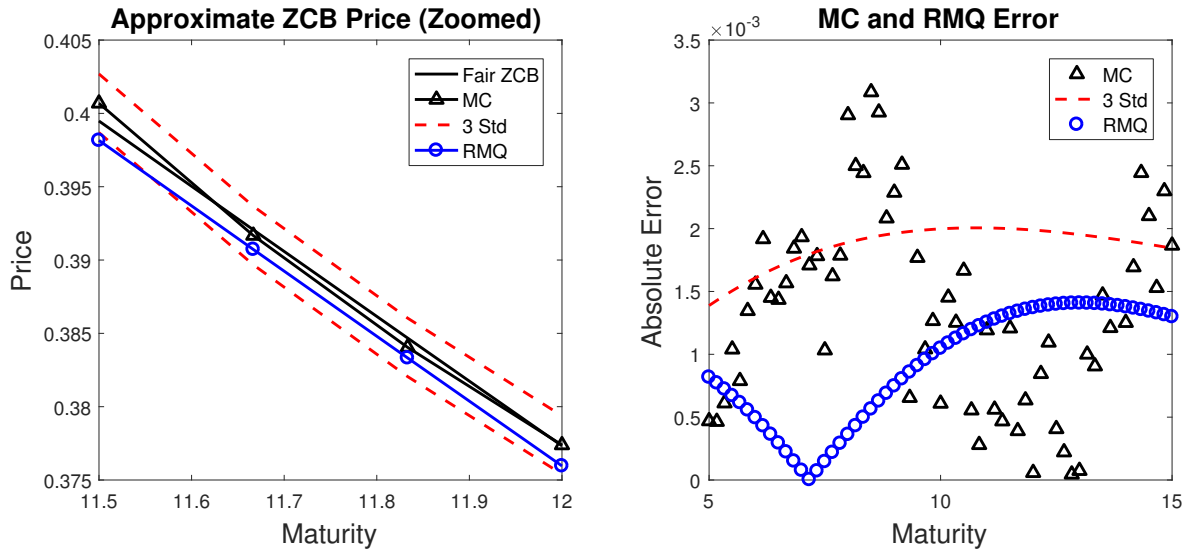


Figure 6: Approximating the fair zero-coupon bond price using Monte Carlo simulation and RMQ.

expensive, under the  $3/2$  dynamics, as the maturity lengthens further. It is beyond the scope of this work to demonstrate the hedging of these contracts. [Hulley and Platen \[2012\]](#) have, however, demonstrated that the theoretical real-world bond prices can be accurately hedged.

In Figure 6 the fair zero coupon bond price is approximated using Monte Carlo simulation and the RMQ algorithm. The Monte Carlo simulation for the IR and MPOR components were each computed using 100 000 paths. The MPOR component could be long-stepped to each maturity considered, as the exact transition density is known, however the  $3/2$  model was simulated using an Euler-Maruyama scheme with 6 time steps per year. The RMQ algorithm also used 6 time steps per year with 50 codewords for the short-rate process and 150 codewords for the discounted GOP process. The Monte Carlo simulation took 13.5 seconds to compute, whereas the RMQ algorithm was more than twice as fast at 5.1 seconds.

The absolute error for both methods is small; the left panel of Figure 6 has been zoomed in to focus on a 6-month period so that the difference between the approximations and the analytic value can be seen. The Monte Carlo method presents some bias over the full period, as more points lie outside the three standard deviation bounds than would be expected. The RMQ algorithm lies well within the error bounds for the full range of maturities.

### 3.2.1 Affect of Short Rate and GOP Correlation

Although the assumption of independence between the short rate and GOP seems restrictive, some empirical evidence is provided for it by [Baldeaux et al. \[2015\]](#). They use the daily 3-month USD T-Bill rates as the proposed short rate and the EWI114 equi-weighted index to approximate the GOP. They find that the covariation remains close to zero and exhibits no clear trend. The theory of approximating the GOP using a well-diversified world-index is presented by [Platen and Rendek \[2012\]](#). It is now demonstrated that the RMQ methodology can also efficiently handle the case of correlation between the short-rate and the GOP.

To account for correlation, the Joint RMQ algorithm, developed by [Rudd et al. \[2017\]](#),

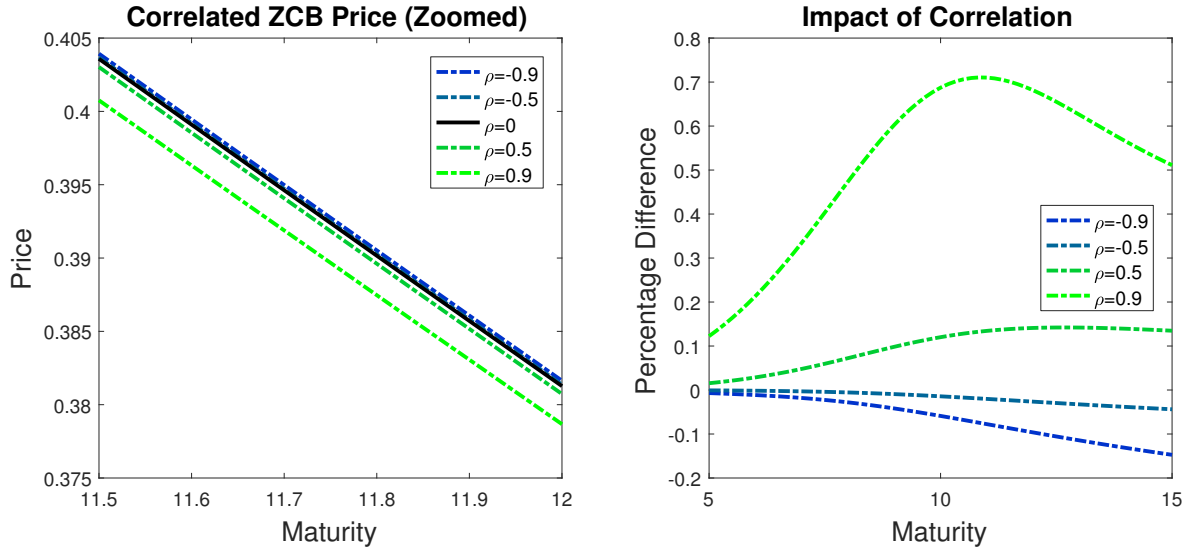


Figure 7: The fair zero-coupon bond price in the hybrid model for a range of correlation values.

has been used. In the left panel of Figure 7 the zero-coupon bond price under the hybrid model is displayed for a range of correlation values between  $-0.9$  and  $0.9$ . The large range is chosen to exaggerate the effect. The impact of positive correlation is greater than that of negative correlation, but the overall impact of the correlation is small. Again, the figure has been zoomed in to focus on a 6-month period. In the right panel of Figure 7 the percentage difference between the zero-coupon bond price and the price with zero correlation is displayed for different correlations and maturities out to 15 years.

These numerical results substantiate the original finding: even for large values of the correlation the impact on the zero-coupon bond price is less than 0.8%. Thus, for bond-pricing applications, correlation between the GOP and the short rate may be safely neglected. Intuitively, the correlation can be viewed as affecting the path of the MPOR process while leaving the path of the IR process unchanged, for example, when running an Euler Monte Carlo simulation with the covariance matrix decomposed using the Cholesky decomposition. However, the path of the MPOR process only has a minimal effect on the zero-coupon bond price for shorter maturities, as seen in the left panel of Figure 6. Thus, changing the correlation only has a small effect on the final zero-coupon bond price.

### 3.2.2 Zero-coupon Bond Options

To price a European put option on a zero-coupon bond, denoted ZCP, under the hybrid model with the option maturing at  $T$  and the bond maturing at  $S > T$ , the following expectation must be computed

$$\text{ZCP}_{T,S,K}(t, r_t, \bar{S}_t^*) := \mathbb{E} \left[ \frac{S_t^*}{S_T^*} (K - P_S(T, r_T, \bar{S}_T^*))^+ \middle| \mathcal{A}_t \right].$$

In Figure 8, the prices obtained using Monte Carlo simulation and the RMQ algorithm for the case  $T = 10$  years and  $S = 15$  years are displayed. The at-the-money strike is taken as the



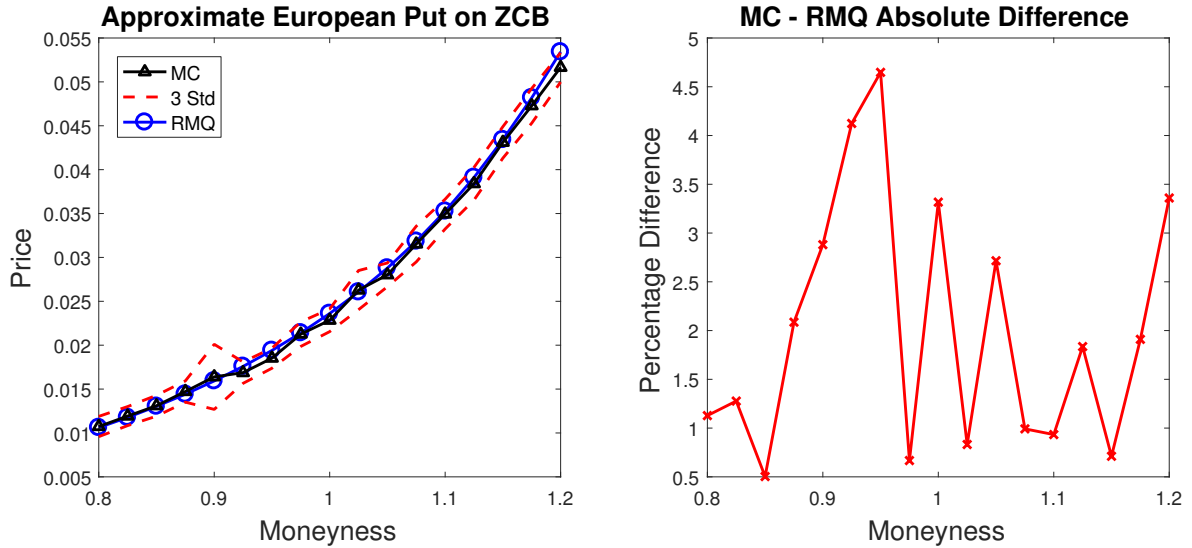


Figure 8: Approximating the prices of a European put on a zero-coupon bond using Monte Carlo simulation and RMQ.

fair forward bond. As before, the Monte Carlo simulation for the IR and MPOR components used 100 000 paths each. The RMQ algorithm used 12 time steps per year with 50 codewords for the short-rate process and 150 codewords for the discounted GOP process. The Monte Carlo simulation took 2.45 seconds per strike, whereas the RMQ algorithm computed the prices for all strikes in 3.6 seconds.

There is no reference price available, but the prices obtained using the RMQ algorithm and Monte Carlo simulation lie sufficiently close together to indicate that RMQ is efficient and accurate. Barring a single deep in-the-money point, all the prices obtained using RMQ lie within the three standard deviation bounds of the Monte Carlo simulation. The average difference between the prices across all strikes is less than 2%.

It has already been established that, under the dynamics of the hybrid model, real-world zero-coupon bonds are less expensive than the bonds implied by traditional risk-neutral pricing. If a risk-neutral measure is assumed, this leads to an asymmetry in the prices of vanilla options on zero-coupon bonds. Real-world put options on fair bonds are more expensive than risk-neutral put options on risk-neutral bonds. The reverse is, of course, true for call options. This behaviour is illustrated in Figure 9 for  $T = 5$  years and  $S = 10$  years. For the example depicted, the fair forward bond was computed using real-world pricing and the same strikes were used for both the real-world and risk-neutral options.

## 4 Conclusion

In this paper, the benchmark approach was reviewed and a derivation of the real-world pricing theorem was presented for a two-asset continuous market. It was demonstrated that real-world pricing may produce significantly lower prices for long-dated bonds and vanilla options than the classical risk-neutral pricing approach. The time-dependent constant elasticity of variance model was used to model the growth-optimal portfolio. Under this model and the assumption

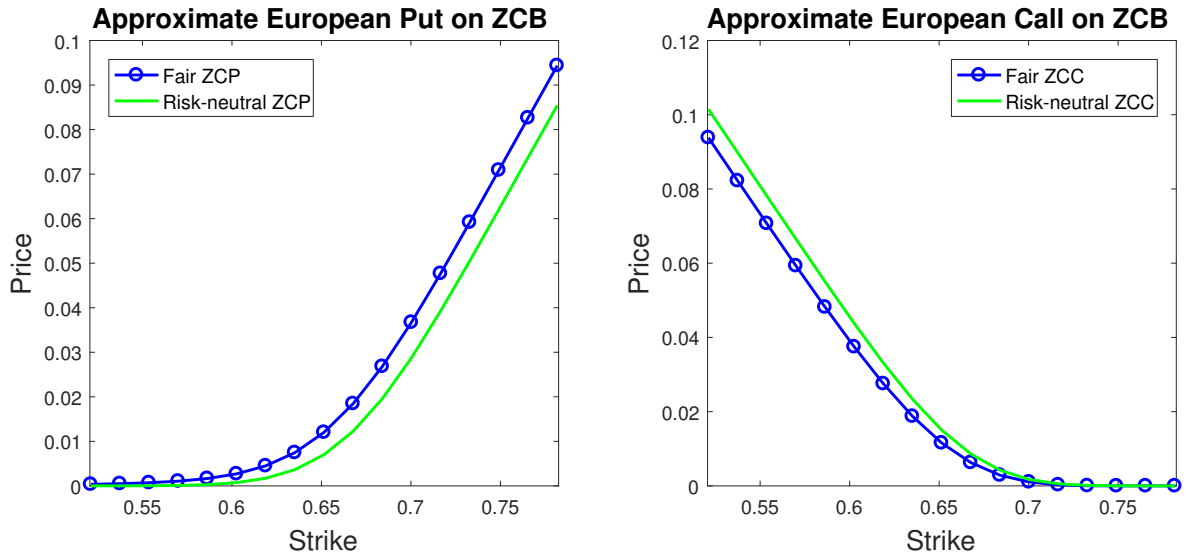


Figure 9: Comparison of European put and call options written on zero-coupon bonds using real-world pricing and priced under a hypothetical risk-neutral measure.

of constant interest rates, analytic European option pricing formulae were derived in detail, extending the results of [Miller and Platen \[2008, 2010\]](#), for the modified constant elasticity of variance model and the stylized minimal market model. Recursive marginal quantization was used to efficiently and accurately produce long-dated European option pricing surfaces as well as price Bermudan options on the growth-optimal portfolio.

The hybrid model of [Baldeaux et al. \[2015\]](#) is constructed by combining the TCEV model, for the growth-optimal portfolio, with the 3/2 short-rate model of [Ahn and Gao \[1999\]](#). Under this combined model, RMQ was used to efficiently price long-dated zero-coupon bonds and options on zero-coupon bonds. The effect of introducing correlation between the growth-optimal portfolio and the stochastic short rate was investigated using the Joint RMQ algorithm, where it was shown that the correlation only has a minor impact.

This paper applied the RMQ algorithm outside the traditional risk-neutral framework by highlighting its effectiveness as a pricing mechanism for long-dated contracts under the benchmark approach.

## References

- D. H. Ahn and B. Gao. A parametric nonlinear model of term structure dynamics. *The Review of Financial Studies*, 12(4):721–762, 1999.
- J. Baldeaux, K. Ignatieva, and E. Platen. A tractable model for indices approximating the growth optimal portfolio. *Studies in Nonlinear Dynamics and Econometrics*, 18(1):1–21, 2014.
- J. Baldeaux, M. C. Fung, K. Ignatieva, and E. Platen. A hybrid model for pricing and hedging of long-dated bonds. *Applied Mathematical Finance*, 22(4):366–398, 2015.
- F. Delbaen and W. Schachermayer. A general version of the fundamental theorem of asset pricing. *Mathematische Annalen*, 300(1):463–520, 1994.
- F. Delbaen and W. Schachermayer. The fundamental theorem of asset pricing for unbounded stochastic processes. *Mathematische Annalen*, 312(2):215–250, 1998.
- W. Feller. Two singular diffusion problems. *Annals of Mathematics*, 54(1):173–182, 1951.
- C. Fontana. Weak and strong no-arbitrage conditions for continuous financial markets. *International Journal of Theoretical and Applied Finance*, 18(01):1550005, 2015.
- H. Geman, N. El Karoui, and J.-C. Rochet. Changes of numeraire, changes of probability measure and option pricing. *Journal of Applied Probability*, 32(2):443–458, 1995.
- N. H. Hakansson and W. T. Ziemba. Capital growth theory. *Handbooks in Operations Research and Management Science*, 9:65–86, 1995.
- D. Heath and E. Platen. Consistent pricing and hedging for a modified constant elasticity of variance model. *Quantitative Finance*, 2(6):459–467, 2002.
- H. Hulley and E. Platen. Hedging for the long run. *Mathematics and Financial Economics*, 6(2):105–124, 2012.
- P. Hunt and J. Kennedy. *Financial Derivatives in Theory and Practice*. John Wiley & Sons, 2004.
- M. Jeanblanc, M. Yor, and M. Chesney. *Mathematical Methods for Financial Markets*. Springer, 2009.
- I. Karatzas and C. Kardaras. The numeraire portfolio in semimartingale financial models. *Finance and Stochastics*, 11(4):447–493, 2007.
- J. Kelly. A new interpretation of information rate. *IRE Transactions on Information Theory*, 3(2):185–189, 1956.
- A. Lindsay and D. Brecher. Simulation of the CEV process and the local martingale property. *Mathematics and Computers in Simulation*, 82(5):868–878, 2012.
- J. B. Long. The numeraire portfolio. *Journal of Financial Economics*, 26(1):29–69, 1990.

- T. A. McWalter, R. Rudd, J. Kienitz, and E. Platen. Recursive marginal quantization of higher-order schemes. *Quantitative Finance*, 2018. doi: 10.1080/14697688.2017.1402125. URL <https://doi.org/10.1080/14697688.2017.1402125>.
- S. M. Miller and E. Platen. Analytic pricing of contingent claims under the real-world measure. *International Journal of Theoretical and Applied Finance*, 11(08):841–867, 2008.
- S. M. Miller and E. Platen. Real-world pricing for a modified constant elasticity of variance model. *Applied Mathematical Finance*, 17(2):147–175, 2010.
- G. Pagès and A. Sagna. Recursive marginal quantization of the Euler scheme of a diffusion process. *Applied Mathematical Finance*, 22(5):463–498, 2015.
- E. Platen. A minimal financial market model. Discussion Papers, Interdisciplinary Research Project 373: Quantification and Simulation of Economic Processes 2000,91, Berlin, 2001. URL <http://hdl.handle.net/10419/62176>. urn:nbn:de:kobv:11-10048178.
- E. Platen. Arbitrage in continuous complete markets. *Advances in Applied Probability*, 34(3): 540–558, 2002.
- E. Platen. Pricing and hedging for incomplete jump diffusion benchmark models. In *AMS-IMS-SIAM Joint Summer Research Conference on Mathematics of Finance*. American Mathematical Society, 2004.
- E. Platen. A benchmark approach to finance. *Mathematical Finance*, 16(1):131–151, 2006.
- E. Platen. Law of the minimal price. Technical report, University of Technology, Sydney. QFRC Research Paper 215, 2008.
- E. Platen and D. Heath. *A Benchmark Approach to Quantitative Finance*. Springer, 2006.
- E. Platen and R. Rendek. Approximating the numeraire portfolio by naive diversification. *Journal of Asset Management*, 13(1):34–50, 2012.
- D. Revuz and M. Yor. *Continuous Martingales and Brownian Motion*. Springer, 1999.
- R. Rudd, T. A. McWalter, J. Kienitz, and E. Platen. Fast quantization of stochastic volatility models. Available at SSRN 2956168, 2017.
- P. A. Samuelson. St. petersburg paradoxes: Defanged, dissected, and historically described. *Journal of Economic Literature*, 15(1):24–55, 1977.
- M. Schroder. Computing the constant elasticity of variance option pricing formula. *Journal of Finance*, 44(1):211–219, 1989.

## Appendix A: Squared Bessel Processes

This appendix summarizes properties of squared Bessel processes that are relevant to real-world pricing.

Introduce  $\mathbf{w} = \{\mathbf{w}_t = (w_t^1, w_t^2, \dots, w_t^n)^\top, t \in [0, \infty)\}$ , as an  $n$ -dimensional standard Brownian motion with  $n \in \mathbb{N}$ . Let the process  $R = \{R_t = |\mathbf{w}_t|, t \in [0, \infty)\}$ , be the Euclidean norm of  $\mathbf{w}$ , such that  $(R_t)^2 = \sum_{i=1}^n (w_t^i)^2$ . Itô's formula provides

$$d(R_t)^2 = n dt + \sum_{i=1}^n 2w_t^i dw_t^i.$$

For any  $t > 0$ ,  $\mathbb{P}(R_t = 0) = 0$ , such that

$$dW_t = \frac{1}{R_t} \sum_{i=1}^n w_t^i dw_t^i$$

is a real-valued Brownian motion via Levý's characterization,<sup>2</sup> and  $R$  satisfies

$$d(R_t)^2 = n dt + 2R_t dW_t.$$

Set  $X_t = (R_t)^2$ . Then, for every  $\delta \in \mathbb{N}$  and  $X_0 = x \geq 0$ , the unique strong solution to the stochastic differential equation

$$dX_t = \delta dt + 2\sqrt{|X_t|} dW_t,$$

is known as a *squared Bessel process* of dimension  $\delta$ , denoted  $\text{BESQ}_t^\delta$ . Although this intuitive derivation accounts only for squared Bessel processes of positive and integer dimension, this can be extended to  $\delta \in \mathbb{R}$  [Revuz and Yor, 1999].

**Definition A.1** ( $\text{BESQ}_t^\delta$ ). *For every  $\delta \in \mathbb{R}$  and  $x \in \mathbb{R}$ , the unique strong solution to*

$$dX_t = \delta dt + 2\sqrt{|X_t|} dW_t, \tag{16}$$

*with  $X_0 = x$ , is called a squared Bessel process of dimension  $\delta$ , starting at  $x$  and denoted by  $\text{BESQ}_t^\delta$ .*

To relate the stochastic differential equations that arise when modelling the growth-optimal portfolio to squared Bessel processes, Proposition 6.3.1.1 of Jeanblanc et al. [2009] is reproduced below.

**Proposition A.1.** *Let  $S = \{S_t, t \in [0, \infty)\}$  be a Cox-Ingersoll-Ross process satisfying*

$$dS_t = \kappa(\theta - S_t) dt + \sigma\sqrt{S_t} dW_t,$$

*with  $S_0 = x \geq 0$  and  $\kappa, \theta > 0$ , and define  $\varphi(t) = \frac{\sigma^2}{4\kappa}(e^{\kappa t} - 1)$ . Then*

$$S_t = e^{-\kappa t} X_{\varphi(t)},$$

*where  $X_{\varphi(t)}$ ,  $\varphi(t) \geq 0$ , is a  $\text{BESQ}_{\varphi(t)}^\delta$  process with dimension  $\delta = \frac{4\kappa\theta}{\sigma^2}$ .*

This allows the square-root process to be expressed as a time-transformed squared Bessel process, for which the transition density is well-understood.

<sup>2</sup>It is a continuous local martingale starting from zero and its quadratic variation is easily verified.

## A.1 The Transition Density of the Squared Bessel Process

Lindsay and Brecher [2012] investigate the transition densities of squared Bessel processes under three different regimes, categorized by the dimension,  $\delta$ . They follow the classic analysis of Feller [1951], who proceeded by solving the Fokker-Planck equation associated with a more general version of (16).

### A.1.1 The case $\delta \leq 0$

When  $\delta \leq 0$ , the  $X = 0$  boundary is attainable and absorbing. The fundamental solution to the associated Fokker-Planck equation is the transition density

$$p_{\delta \leq 0}(X_T, T; X_0) = \frac{1}{2T} \left( \frac{X_T}{X_0} \right)^{\frac{1}{2}(\frac{\delta}{2}-1)} \exp\left(-\frac{X_T + X_0}{2T}\right) I_{1-\frac{\delta}{2}}\left(\frac{\sqrt{X_T X_0}}{T}\right), \quad (17)$$

where  $I_\nu(x)$  is a modified Bessel function of the first kind with index  $\nu$ . By inspection, the above is related to the noncentral chi-squared density,

$$p_{\delta \leq 0}(X_T, T; X_0) = \frac{1}{T} p_{\chi'^2}\left(\frac{X_0}{T}; 4 - \delta, \frac{X_T}{T}\right), \quad (18)$$

expressed as a function of the noncentrality parameter, such that

$$\begin{aligned} \int_x^\infty p_{\delta \leq 0}(X, T; X_0) dX &= \int_x^\infty p_{\chi'^2}\left(\frac{X_0}{T}; 4 - \delta, \frac{X}{T}\right) dX \\ &= \chi'^2\left(\frac{X_0}{T}; 2 - \delta, \frac{x}{T}\right). \end{aligned} \quad (19)$$

The final step above was shown by Schroder [1989].

This density is, however, *norm-decreasing*,

$$\int_0^\infty p_{\delta \leq 0}(X, T; X_0) dX = \chi'^2\left(\frac{X_0}{T}; 2 - \delta, 0\right) \leq 1, \quad (20)$$

as it does not include the probability of the process being absorbed at zero. Lindsay and Brecher [2012] propose constructing a full, norm-preserving density by adding a Dirac mass at the origin,

$$p_{\delta \leq 0}^{\text{full}}(X_T, T; X_0) := 2 \left(1 - \chi'^2\left(\frac{X_0}{T}; 2 - \delta, 0\right)\right) \bar{\delta}(X_T) + p_{\delta \leq 0}(X_T, T; X_0), \quad (21)$$

where  $\bar{\delta}(x)$  is the Dirac delta function. Then the distribution of  $X$  is given by

$$\mathbb{P}(X \leq X_T | X_0) = \int_0^{X_T} p_{\delta \leq 0}^{\text{full}}(X, T; X_0) dX = 1 - \chi'^2\left(\frac{X_0}{T}; 2 - \delta, \frac{X_T}{T}\right). \quad (22)$$

### A.1.2 The case $0 < \delta < 2$

When  $0 < \delta < 2$ , the  $X = 0$  boundary is attainable and can be either absorbing or reflecting. If an absorbing boundary is selected, the analysis of the previous section holds,

$$p_{0 < \delta < 2}^A(X_T, T; X_0) := p_{\delta \leq 0}^{\text{full}}(X_T, T; X_0).$$

If a reflecting boundary is selected, the sign of the index of the Bessel function in the density changes,

$$\begin{aligned} p_{0 < \delta < 2}^R(X_T, T; X_0) &= \frac{1}{2T} \left( \frac{X_T}{X_0} \right)^{\frac{1}{2}(\frac{\delta}{2}-1)} \exp\left(-\frac{X_T + X_0}{2T}\right) I_{\frac{\delta}{2}-1}\left(\frac{\sqrt{X_T X_0}}{T}\right) \\ &= \frac{1}{T} p_{\chi'^2}\left(\frac{X_T}{T}; \delta, \frac{X_0}{T}\right), \end{aligned} \quad (23)$$

such that it is directly related to the non-central chi-squared density without the reversal of the roles of  $X_T$  and  $X_0$  seen in the  $\delta \leq 0$  case in (18). This density is clearly norm-preserving.

### A.1.3 The case $\delta > 2$

When  $\delta > 2$ , the process can not attain zero and thus no boundary conditions can be specified. The transition density is of the same type as in the reflecting case,

$$p_{\delta > 2}(X_T, T; X_0) = \frac{1}{T} p_{\chi'^2}\left(\frac{X_T}{T}; \delta, \frac{X_0}{T}\right). \quad (24)$$

### A.1.4 Symmetry Relationships

When  $\delta > 2$ , the transition density is given by (24). When considering only an absorbing boundary, for all  $\delta < 2$ , the norm-decreasing part of the transition density is given by (17). A simple symmetry relationship exists between these two expressions,

$$p_\delta(X_T, T; X_0) = p_{4-\delta}(X_0, T; X_T), \quad (25)$$

that aids in the option pricing problems considered in the paper.

Furthermore,

$$X_T^{(1-\frac{\delta}{2})} p_\delta(X_T, T; X_0) = X_0^{(1-\frac{\delta}{2})} p_\delta(X_0, T; X_T) = X_0^{(1-\frac{\delta}{2})} p_{4-\delta}(X_T, T; X_0). \quad (26)$$

The first equation follows from simple arithmetic using either (23) or (17) and the second equation follows from the first symmetry relationship above, (25).

An important implication of the above result is that if  $X$  is a BESQ $^\delta$  process with  $\delta > 2$  and  $X_0 > 0$ , the process  $Z_t = X_t^{(1-\frac{\delta}{2})}$  is a *strict* local martingale<sup>3</sup>. This follows because the integral of the last term above is strictly less than one:

$$\begin{aligned} \mathbb{E}[Z_T] &= \int_0^\infty X^{(1-\frac{\delta}{2})} p_{\delta > 2}(X, T; X_0) dX \\ &= \int_0^\infty X_0^{(1-\frac{\delta}{2})} p_{(4-\delta) < 2}(X_0, T; X) dX \\ &= X_0^{(1-\frac{\delta}{2})} \chi'^2\left(\frac{X_0}{T}; \delta - 2, 0\right) \\ &< Z_0. \end{aligned}$$

---

<sup>3</sup>In fact it is a supermartingale, by Fatou's lemma, as it is bounded below